THE JOURNAL OF BIOLOGICAL CHEMISTRY VOL. 288, NO. 47, pp. 34030–34040, November 22, 2013
Published in the U.S.A.

Agonist-induced Ca^{2+} Sensitization in Smooth Muscle

REDUNDANCY OF RHO GUANINE NUCLEOTIDE EXCHANGE FACTORS (RhoGEFs) AND RESPONSE KINETICS, A CAGED COMPOUND STUDY[*] [S]

Received for publication, August 30, 2013, and in revised form, October 4, 2013 Published, JBC Papers in Press, October 8, 2013, DOI 10.1074/jbc.M113.514596

Mykhaylo V. Artamonov[‡], Ko Momotani[‡], Andra Stevenson[§], David R. Trentham[¶], Urszula Derewenda[‡], Zygmunt S. Derewenda[‡], Paul W. Read[‖], J. Silvio Gutkind[**], and Avril V. Somlyo[‡1]

From the Departments of [‡]Molecular Physiology and Biological Physics and [‖]Radiation Oncology, University of Virginia, Charlottesville, Virginia 22908, [§]Department of Cardiovascular Diseases, Merck Research Laboratories, Kenilworth, New Jersey 07033, [¶]The Randall Division of Cell and Molecular Biophysics, School of Biomedical Sciences, King's College London, London SE1 1UK, United Kingdom, and [**]Oral and Pharyngeal Cancer Branch, NIDCR, National Institutes of Health, Bethesda, Maryland 20892

Background: Multiple RhoGEFs regulate agonist-induced Ca^{2+}-sensitized force.
Results: PDZRhoGEF and LARG are functionally redundant, translocate to the cell membrane, and form hetero- and homodimers to mediate $G\alpha_{12/13}$-dependent RhoA activation.
Conclusion: Ca^{2+}-sensitized force is induced by parallel signaling through RhoGEFs, which are rate-limiting due to their slow recruitment and activation.
Significance: Signaling through RhoGEFs suggests new therapeutic targets for diseases of smooth muscle.

Many agonists, acting through G-protein-coupled receptors and Gα subunits of the heterotrimeric G-proteins, induce contraction of smooth muscle through an increase of $[Ca^{2+}]_i$ as well as activation of the RhoA/RhoA-activated kinase pathway that amplifies the contractile force, a phenomenon known as Ca^{2+} sensitization. $G\alpha_{12/13}$ subunits are known to activate the regulator of G-protein signaling-like family of guanine nucleotide exchange factors (RhoGEFs), which includes PDZ-RhoGEF (PRG) and leukemia-associated RhoGEF (LARG). However, their contributions to Ca^{2+}-sensitized force are not well understood. Using permeabilized blood vessels from PRG(−/−) mice and a new method to silence LARG in organ-cultured blood vessels, we show that both RhoGEFs are activated by the physiologically and pathophysiologically important thromboxane A_2 and endothelin-1 receptors. The co-activation is the result of direct and independent activation of both RhoGEFs as well as their co-recruitment due to heterodimerization. The isolated recombinant C-terminal domain of PRG, which is responsible for heterodimerization with LARG, strongly inhibited Ca^{2+}-sensitized force. We used photolysis of caged phenylephrine, caged guanosine 5′-*O*-(thiotriphosphate) (GTPγS) in solution, and caged GTPγS or caged GTP loaded on the RhoA·RhoGDI complex to show that the recruitment and activation of RhoGEFs is the cause of a significant time lag between the initial Ca^{2+} transient and phasic force components and the onset of Ca^{2+}-sensitized force.

Contraction of smooth muscle (SM)[2] is responsible for critical bodily functions, including the maintenance of proper blood pressure within the vasculature. It is well established that agonists such as angiotensin, epinephrine, endothelin-1 (ET-1), thromboxane A2 (TXA2), etc. induce SM contraction through G-protein-coupled receptors (GPCRs) and Gα subunits of the heterotrimeric G-proteins (1). Stimulation of the receptors initiates two parallel signaling pathways: an influx of Ca^{2+}, both through dedicated channels and release from intracellular storage, and activation of the RhoA/RhoA-activated kinase (ROCK) pathway, which amplifies the Ca^{2+}-induced contractile force (also known as Ca^{2+} sensitization) (2). The increase in $[Ca^{2+}]_i$ leads to activation of the myosin light chain kinase by the Ca^{2+}·calmodulin complex, and subsequent phosphorylation of the myosin regulatory light chain (RLC_{20}) (3). ROCK phosphorylates and inhibits the MYPT1 subunit of the myosin light chain phosphatase (MLCP), increasing the phosphorylation level of RLC_{20} and consequently amplifying the contractile force (4, 5). The physiology of these events is of profound medical significance because misregulation of RhoA signaling results in abnormalities of SM function such as hypertension, asthma, cerebral and coronary vasospasm, preterm labor, disturbed gut motility, and erectile dysfunction as reviewed elsewhere (6).

Although the mechanism of Ca^{2+}-mediated induction of force is relatively well understood, the molecular pathways involved in Ca^{2+} sensitization are less clear largely because of the degenerate nature of the signaling routes. Agonist-activated GPCRs are coupled to various Gα subunits, including $G\alpha_{12/13}$

* This work was supported, in whole or in part, by National Institutes of Health Grants GM086457 and R01DK088905.
[S] This article contains supplemental Experimental Procedures, Figs. 1–7, and Table 1.
[1] To whom correspondence should be addressed: Dept. of Molecular Physiology and Biological Physics, University of Virginia, P. O. Box 736, Charlottesville, VA 0736-22908. Tel.: 434-982-0825; Fax: 434-982-1616; E-mail: avs5u@virginia.edu.

[2] The abbreviations used are: SM, smooth muscle; ET-1, endothelin-1; GAP, GTPase-activating protein; GDI, guanine nucleotide dissociation inhibitor; GPCR, G-protein-coupled receptor; LARG, leukemia-associated RhoGEF; Lbc, lymphoid blast crisis; MLCP, myosin light chain phosphatase; MYPT1, myosin-targeting phosphatase subunit 1; ROCK, RhoA-activated kinase; PRG, PDZRhoGEF; GEF, guanine nucleotide exchange factor; RLC_{20}, regulatory light chain; TXA2, thromboxane A2; GTPγS, guanosine 5′-*O*-(thiotriphosphate); kd, knockdown.

and $G\alpha_{q/11}$, which in turn interact with and activate a range of guanine nucleotide exchange factors for Rho family GTPases (RhoGEFs) that catalyze the GDP to GTP exchange on RhoA (7). Once loaded with GTP, RhoA is capable of binding to and activating ROCK (6). Of the 74 known Dbl homology GEFs found in the human genome, a significant number are known to act on RhoA (8), and a number of them are expressed in SM cells, but it is not known exactly how many are functional and how they are coupled to GPCRs. One possibility is that by acting on specific GPCRs different agonists initiate signaling along unique pathways mediated by specific RhoGEFs (1). Thus, for example, the leukemia-associated RhoGEF (LARG), which acts through $G\alpha_{12/13}$, was implicated uniquely to control salt-induced hypertension but not the maintenance of basal blood pressure (9). Also, we and others have discovered that $G\alpha_{q/11}$ activates p63RhoGEF and that this route may be important for agonists acting on GPCRs coupled to $G\alpha_{q/11}$ such as ET-1 and angiotensin (10–12). However, it is possible that two or more RhoGEFs respond to agonist stimulation either through the same or different $G\alpha$ subunits. Each agonist may stimulate one or more GPCRs, and this may potentially lead to activation of various RhoGEFs with different catalytic activities and potentially different activation times. If this is true, then the balance of the Ca^{2+}-induced and Ca^{2+}-sensitized components of the contractile response may vary considerably between agonists, and the same could be true of the time course of the Ca^{2+}-sensitized response. In this study, we probed both the potential redundancy of RhoGEFs downstream of the $G\alpha$-mediated signaling in SM and the nature of the time lag associated with the onset of Ca^{2+}-sensitized force following Ca^{2+}-induced transient phase.

We focused on a family of RhoGEFs known to be activated by $G\alpha_{12/13}$ that includes LARG (13), PDZRhoGEF (hereafter referred to as PRG) (14), and p115RhoGEF (15), all of which contain the regulator of G-protein signaling-like domain that mediates the interaction (16). The $G\alpha_{12/13}$ subunits are coupled to several GPCRs that are activated by potent vasoconstricting agonists such as TXA2 and ET-1, and so in principle each agonist could activate all three RhoGEFs. However, it has been established that SM of p115RhoGEF(−/−) mice develops normal contraction when stimulated by ET-1 and TXA2 (17), and so we pursued the question as to whether PRG and LARG are activated together. Unfortunately, the combined PRG(−/−) and LARG(−/−) knock-out is lethal (18), so we took advantage of a unique procedure that allowed us to silence LARG in organ-cultured blood vessels derived from both normal and PRG(−/−) mice (18). To our knowledge, this is the first study of this kind to be reported for SM vessels. Using canonical contractility assays we determined that SM tissue samples derived from the doubly genetically modified vessels show much more deficient Ca^{2+} sensitization than either the PDZ(−/−) or LARG knockdown ($LARG^{kd}$) SM samples. Moreover, we present data supporting the notion that this functional redundancy is caused by both direct activation of the two RhoGEFs and their co-recruitment due to heterodimerization. Finally, tissues deficient in either PRG or LARG showed significantly delayed onset of ET-1-induced Ca^{2+}-sensitized force and required a much longer time to reach maximum contraction. We explored this further by directly measuring times to activation using photolysis of caged phenylephrine, caged GTPγS in the bath solution, and caged GTPγS or caged GTP loaded on the RhoA·RhoGDI complex or on the G14V RhoA·RhoGDI complex, respectively, to show that the recruitment and activation of RhoGEFs is the cause of a significant time lag between the initial Ca^{2+} transient and phasic force components and the onset of Ca^{2+}-sensitized force. Our data strongly suggest that that activation of RhoGEFs is rate-limiting for Ca^{2+} sensitization of SM.

EXPERIMENTAL PROCEDURES

All procedures using animals were carried out according to protocols approved by the Animal Care and Use Committee at the University of Virginia.

Generation of PRG(−/−) Mice—The generation, genotyping, and characterization of the PRG(−/−) knock-out mice have been described in detail elsewhere (18). The lack of PRG expression is documented in supplemental Fig. 1. Other details are provided in the supplemental Experimental Procedures.

Reverse Transcription-Polymerase Chain Reaction (RT-PCR) Screen for RhoGEF mRNA—mRNA was purified from primary mouse aortic cells and SM tissues, and quantitative RT-PCR was performed with primers shown in supplemental Table 1 as described in the supplemental Experimental Procedures.

Adenoviral Transfection of siRNAs into Tissues in Organ Culture and Cultured SM Cells—The construction of shRNA plasmids for suppression of LARG and their characterization are detailed in the supplemental Experimental Procedures. Using an adenoviral construct we developed a method to deliver shRNA to the SM cells in blood vessels. We used a plasmid-based system designated as pMighty in which a specific LARG sequence was inserted downstream of the H1 promoter (19). Replication-deficient adenoviruses encoding the LARG shRNA were generated by the Gene Transfer Vector Core (University of Iowa). A nuclearly targeted LacZ reporter was incorporated into the virus to monitor infection of SM cells using β-galactosidase staining. Treatment of the vessels is detailed in the supplemental Experimental Procedures. Murine portal vein and cerebral arteries, but not upper mesenteric artery, showed a high level of viral infection in SM cells throughout the vessel media (Fig. 1). Portal vein was chosen for silencing LARG and for contractility assays in preference to cerebral arteries because of experimental difficulties when working with small vessels. The effectiveness of the pAd5-Mighty LARG shRNA-containing virus was first tested on primary cultures of mouse and rat aortic SM cells, which showed a suppression of LARG expression by ~70 and ~60%, respectively (supplemental Figs. 2 and 3). Next, we conducted infection of WT and PRG-null mouse portal veins in organ culture and in both cases observed a reduction in LARG levels by ~65% (Fig. 2). The ability of the contractile apparatus in intact vessels to develop force in response to a depolarizing stimulus with high $[K^+]$ was not different from wild-type portal veins, indicative of normal depolarization-induced Ca^{2+} release and RLC_{20} phosphorylation (supplemental Fig. 4).

Tissue Preparation and Force Measurements—Mouse or rabbit portal veins were dissected, denuded of endothelium, cut into small strips (150–250 μm wide, 2–3 mm long), and mounted on a bubble plate or on a wire myograph system for

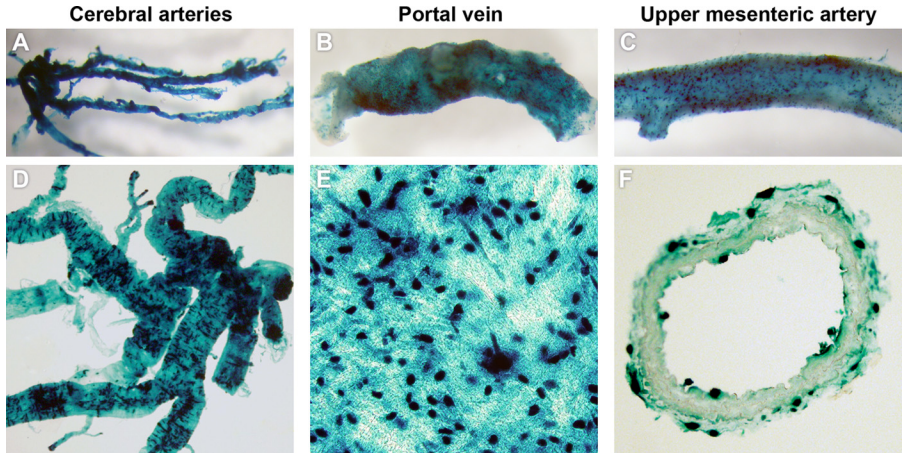

FIGURE 1. **Silencing of protein expression in blood vessels using adenoviral constructs.** Adenoviral constructs for silencing RNAs and protein expression can be successfully introduced into murine portal and cerebral vessels in organ culture. Vessels were incubated with 10^{10} pfu of pAd5-Mighty shRNA targeting LARG with a nuclear LacZ-expressing adenovirus for 48 h as detailed under "Experimental Procedures." *A*, *B*, *D*, and *E*, LacZ reporter was detected by β-galactosidase histochemistry in SM cells across the vessel wall in mouse portal vein and cerebral arteries. *C* and *F*, upper mesenteric arteries showed only superficial infection. LacZ-stained mouse cerebral arteries (A and D), mouse portal vein (*B*) with a transverse section (*E*), and mouse upper mesenteric artery (*C*) with a transverse section (*F*) are shown. Magnification, 6× in *upper panels* and 20× in *lower panels*.

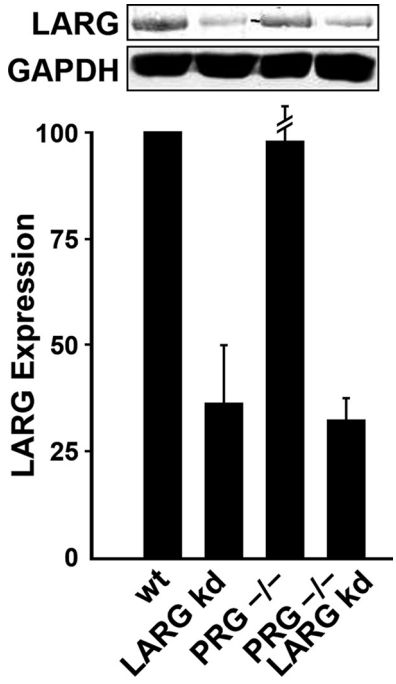

FIGURE 2. **Reduction of LARG protein in WT and PRG-null portal veins following infection with an adenoviral LARG-targeted shRNA construct.** LARG protein expression was significantly suppressed with shRNA targeting LARG but not with a non-targeting control in the portal vein strips pooled from three to four mice following contractile measurements. The *errors bars* correspond to S.E.; $n = 3–4$.

force measurements (20) or in a muscle trough for photolysis experiments (21). The magnitude of contraction with 154 mM K^+ was measured prior to stimulation with different agonists (20). Following force measurements, muscle strips were pooled for biochemical analysis. For Ca^{2+} sensitization experiments, mouse portal veins were permeabilized with α-toxin (1,500 units/ml) and treated with 10 μM A23187 and with NO synthase inhibitor L-N^G-nitroarginine methyl ester. Ca^{2+}-buffered solutions are detailed in the supplemental Experimental Procedures. Muscle strips were exposed to Ca^{2+} clamped at *p*Ca 6.7–6.3, and once the force reached a plateau, strips were Ca^{2+}-sensitized by an appropriate agonist. Force was normalized to a maximum Ca^{2+}-induced force (*p*Ca 4.5), taken as 100% of potential contractile force. For photolysis experiments, muscles were permeabilized with 75 μM β-escin in G1 solution as detailed in the supplemental Experimental Procedures. Experiments were performed at 22 °C.

Apparatus and Photolysis Techniques—The UV laser for laser flash photolysis, a computer-controlled muscle trough system for solution exchange, the force transducer, and the data collection system have been described in detail previously (21, 22). Protocols for Ca^{2+} measurements, loading of the AM ester of Fluo3 into intact portal vein, pretreatment with cyclopiazonic acid, and introduction of caged compounds and their photolysis are described in the supplemental Experimental Procedures. The rate constant of decay of the *aci*-nitro intermediate of 1-(2-nitrophenyl)ethyl esters of nucleotides (23) following a laser flash was used as a measure of the rate of photolysis of the complexes of caged nucleotides with RhoA·RhoGDI (supplemental Fig. 5). The apparatus was modified as described in the supplemental Experimental Procedures.

Caged Nucleotide-RhoA·RhoGDI Complex—Human RhoA or the constitutively active G14V RhoA mutant were co-expressed with the cytosolic inhibitory protein RhoGDI in *Saccharomyces cerevisiae*. The expression and purification were described in detail elsewhere (24). Caged GTP or GTPγS was exchanged into the complexes as described previously for GTP (24). In the case of caged GTP, the *R*-diastereoisomer was used for the exchange (25, 26). Bound nucleotides were determined by HPLC and quantified as described in the supplemental Experimental Procedures. Final concentrations of caged nucleotides in complexes with RhoA·RhoGDI were in the range of 100–300 μM with 50–75% of the desired nucleotide exchanged into the complex. Following photolysis, 30 μl of the solution was collected, and the fraction of photolyzed nucleotide was quantified by HPLC. Under the experimental conditions used here, an average 8% photolysis yield (range, 3.5–16%) was determined for the caged GTP, caged GTPγS, and both caged nucleotide-loaded RhoA·RhoGDI complexes.

Expression and Purification of Recombinant Proteins—Mouse PRG cDNA (clone NM001003912), either full-length or its relevant segments, was amplified and introduced into pHis-Parallel1 (27) for recombinant protein production in *Escherichia coli* and p3xFLAG-Myc-CMV-24 (Sigma-Aldrich) to express FLAG-tagged PRG in mammalian cells. Mouse LARG cDNA (GI28972190) was introduced into pCMV-Tag 1 mammalian expression vector (Stratagene). His-tagged PRG(1207–1553), PRG(1207–1453), PRG(1207–1553) S1508A/S1510A double mutant, and PRG(1207–1553) S1508E/S1510E double mutant recombinant proteins were produced in *E. coli* BL21-CodonPlus(DE3)-RIPL and purified as detailed in the supplemental Experimental Procedures.

Cell Culture and Cell Transfection—Culture and transfection of HEK 293T and rat aortic SM cells and isolation of WT and PRG(−/−) mouse aortic SM cells are detailed in the supplemental Experimental Procedures.

MLCP and RLC_{20} Phosphorylation—Portal veins treated with control or LARG shRNA, permeabilized, and stimulated with ET-1 (100 nM) or U46619 (300 nM) were analyzed for phosphorylation of MYPT1 at Thr-696/853 and of RLC_{20} at Ser-19 as described previously (28) and shown in supplemental Fig. 6.

Tissue Screen, Western Blots, and Immunofluorescence Staining—SM tissues and cultured cells were lysed in radioimmune precipitation assay buffer or rhotekin assay lysis buffer and used in SDS-PAGE and Western blot. Procedures and antibodies used are given in the supplemental Experimental Procedures. For immunofluorescence microscopy of PRG(+/−) mouse cerebral arteries, see the supplemental Experimental Procedures.

Caged Compounds—Caged phenylephrine (mixed diastereoisomers of *O*-1-(3,4-dimethoxy-6-nitrophenyl)ethyl phenylephrine, derivatized on the phenolic oxygen of phenylephrine) was synthesized essentially as for *O*-1-(2-nitrophenyl)ethyl phenylephrine (29, 30): mass $[M + H]^+$ found, 377.1 Da; calculated, 377.17 Da. The extent of photolysis was estimated by comparing the tension development following photolysis of various concentrations of caged phenylephrine with a dose-response curve for phenylephrine in rabbit portal vein. For comparable tension levels, a photolysis yield of ~8% was estimated with a postphotolysis EC_{50} for phenylephrine of 0.2 μM. Caged GTPγS alkylated on sulfur (*S*-(1-(2-nitrophenyl)ethyl-caged GTPγS) was synthesized (31) or was purchased from Invitrogen. Caged GTP (the single diastereoisomer, (*R*)-P^3-1-(2-nitrophenyl)ethyl ester, of GTP) was used (25, 26). The preparations of caged nucleotide-bound RhoA·RhoGDI complexes are described in the supplemental Experimental Procedures.

Statistical Analysis—Mean values and errors (S.E.) were obtained from three to eight independent measurements for each experiment. The statistical significance of group differences was assessed using Student's *t* test. A p value of <0.05 was considered significant. A p value of >0.05 was considered not significant.

RESULTS

Ca^{2+}-sensitized Force in Normal and Genetically Modified Portal Veins—To assess the physiological role of the LARG and PRG exchange factors in $G\alpha_{12/13}$-mediated Ca^{2+} sensitization in SM, we conducted canonical measurements of the contractile force induced by the agonists ET-1 and U46619, a stable analog of TXA2, using normal and genetically modified samples from mouse portal veins. The genetically altered samples included those obtained from the PRG(−/−) mouse, normal samples in which LARG was knocked down ($LARG^{kd}$) by ~65%, and PRG(−/−) samples in which LARG was knocked down. To confirm that the PRG(−/−) mouse did not show compensating changes in the expression patterns of other prevalent RhoGEFs that may have biased our results, we tested transcription levels of GEF-H1, p63RhoGEF, GEF17, Lbc, LARG, and p115RhoGEF. The mRNA levels did not differ from those found in the tissues of normal animals (Fig. 3*A*). LARG, p115RhoGEF, and p63RhoGEF protein expression levels were also similar in both animals as were those for $G\alpha_{q/11}$, $G\alpha_{12}$, $G\alpha_{13}$, and TXA2 and ET-1 receptors (Fig. 3, *B* and *C*). We concluded that any differences in Ca^{2+}-sensitized force between vessels from the two animals are due to the absence of PRG.

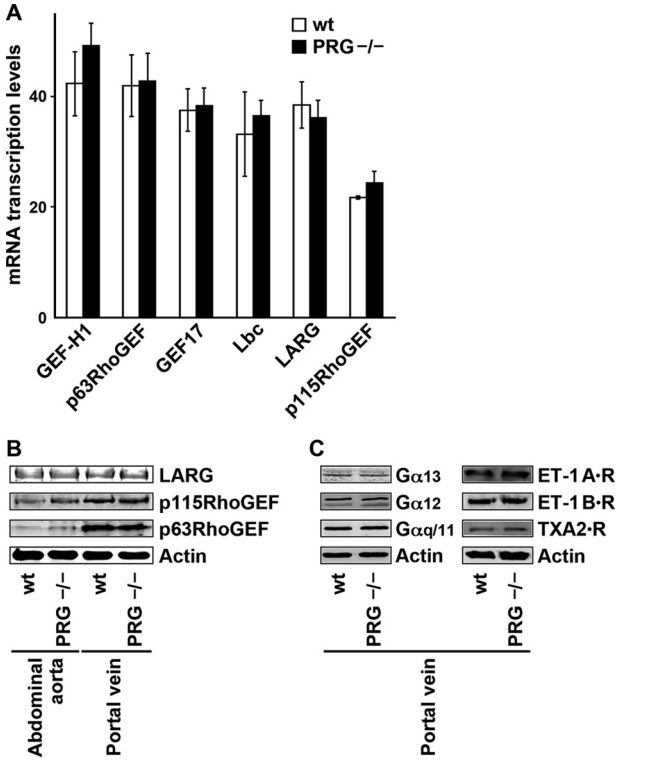

FIGURE 3. **Smooth muscle from PRG-deficient mice does not exhibit compensatory changes in expression of GEF-H1, p63RhoGEF, GEF17, Lbc, LARG, p115RhoGEF,$G\alpha_{q/11}$, $G\alpha_{12}$, $G\alpha_{13}$, and TBXA2 and ET-1 receptors (*R*).** *A*, mRNA transcription profiles of the most abundant RhoGEFs are not significantly different in WT and PRG(−/−) mouse portal veins ($n = 3$). *B*, protein expression of regulator of G-protein signaling GEFs LARG and p115RhoGEF and of p63RhoGEF does not differ in WT and PRG(−/−) mouse blood vessels. *C*, protein expression of PRG upstream receptors for TXA2 and ET-1B as well as of $G\alpha_{q/11}$, $G\alpha_{12}$, and $G\alpha_{13}$ does not differ in WT and PRG(−/−) mouse portal veins. Vessels from three mice were pooled to get enough material for analysis. The *error bars* correspond to S.E. of a minimum of three independent experiments.

In the first series of experiments, we conducted experiments using *intact* mouse portal veins where agonist stimulation initiates a full physiological response, including Ca^{2+}-mediated phosphorylation of RLC_{20} as well as activation of RhoA/ROCK-mediated inhibitory phosphorylation of MLCP (supplemental Fig. 6). Upon stimulation with U46619, knockdown of LARG

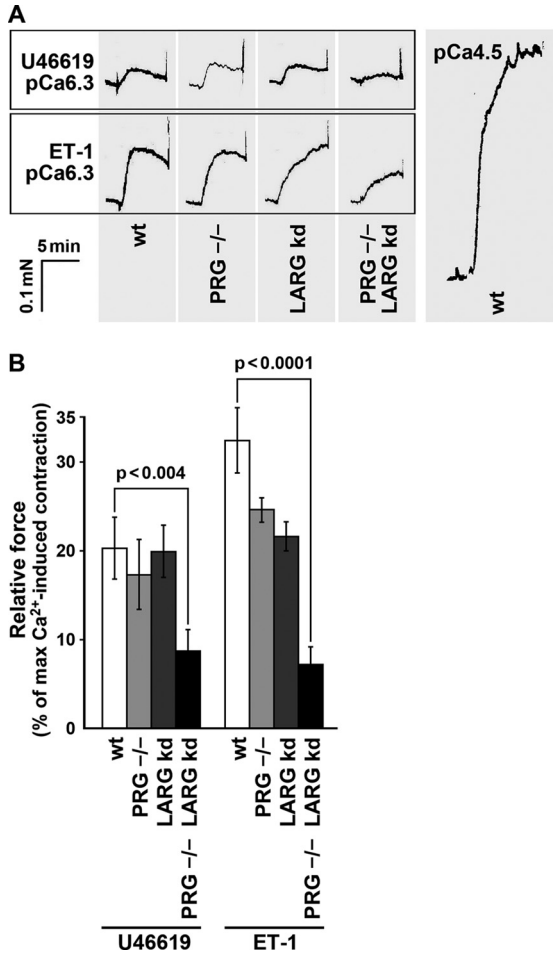

FIGURE 4. **Knockdown of LARG in PRG-null portal vein markedly suppressed TBXA2- and endothelin-1-induced Ca^{2+}-sensitized force to a greater extent than either alone.** *A*, representative force traces from α-toxin-permeabilized WT and PRG-null mouse portal veins infected with adenovirally coupled shRNA targeting LARG or a non-targeting control shRNA. Muscles were stimulated with 300 nM U46619 (*upper panel*) or 50 nM ET-1 (*lower panel*). [Ca^{2+}] was clamped to *p*Ca 6.3. *p*Ca 4.5 is shown as a reference for maximal force. *B*, summary of force developed by U46619 or ET-1 in portal veins from $LARG^{kd}$, PRG(−/−), and double $LARG^{kd}$/PRG(−/−). The force is normalized to maximal force (*p*Ca 4.5). The *error bars* correspond to S.E.; 8–16 muscle strips from four to five mice were used for each group.

alone did not affect the contractile force at maximum agonist concentration, whereas the PRG(−/−) veins showed ~15% reduction under the same condition (supplemental Fig. 7). In the case of ET-1 stimulation, both samples showed ~10% reduction in force at maximum dosage. As expected, the $LARG^{kd}$/PRG(−/−) veins were affected the most with maximum force reduced by ~30% when U46619 was used and by ~20% when ET-1 was used as the agonist (supplemental Fig. 7).

In the second set of experiments, we used permeabilized portal veins in which $[Ca^{2+}]_i$ was clamped with the EGTA buffer. This allowed us to assess the impact of genetic modifications specifically on Ca^{2+} sensitization. At *p*Ca 6.3, the magnitude of the Ca^{2+}-sensitized contractile response to U46619 was virtually unaffected by either the PRG knock-out or LARG knockdown (Fig. 4). However, experiments with the $LARG^{kd}$/PRG(−/−) muscle strips showed a response that was reduced on average to ~40% of that observed for the normal muscle strip. A similar effect was observed in experiments where ET-1 was used as an agonist, although in this case, both the PRG(−/−) and $LARG^{kd}$ strips had reduced contractile responses (~70 and ~75%, respectively, of the response of a normal tissue). The $LARG^{kd}$/PRG(−/−) vein showed only ~25% of the response of the normal sample. To ascertain that the observed differences in Ca^{2+}-sensitized contractility are consistent with the expected biochemical changes, we assayed the levels of phosphorylated RLC_{20} and MYPT1. We found that the impairment of Ca^{2+}-sensitized contractility of vessels from $LARG^{kd}$/PRG(−/−) mice was associated with a significant decrease in phosphorylation of MYPT1 at the ROCK site, Thr-853 (by ~30 and ~60% in U46619- and ET-1-stimulated vessels, respectively), and of RLC_{20} at Ser-19 (~40 and ~55%, respectively) (Fig. 5).

LARG and PRG Are Co-recruited in Response to Agonist Stimulation—It is well established that PRG and LARG form homo- and heterodimers in which the binary interactions are mediated by the C-terminal domains, specifically their coiled coil segments (32, 33). Dimerization does not affect the nucleotide exchange activity nor does the interaction with $G_{\alpha 12/13}$ affect dimerization (33). First, we co-expressed FLAG-tagged full-length PRG and Myc-tagged full-length LARG and performed immunoprecipitation using anti-FLAG antibody-conjugated beads. We observed co-immunoprecipitation of Myc-tagged LARG (Fig. 6*A*). We also co-expressed FLAG-tagged full-length PRG and Myc-tagged full-length PRG and performed immunoprecipitation using anti-Myc antibody-conjugated beads. We observed co-immunoprecipitation of FLAG-tagged PRG. In both cases, no co-immunoprecipitation occurred in the absence of epitope-tagged partners corresponding to antibody-conjugated beads. We wondered whether the heterodimerization might play a role in Ca^{2+}-sensitized force. We hypothesized that the isolated dimerization domain from PRG (residues 1207–1553), but not its truncated variant (residues 1207–1453) lacking the C-terminal coiled coil, might interfere with homo- and heterodimerization and affect Ca^{2+} sensitization. Indeed, a recombinant C-terminal domain, but not a control lacking the coiled coil region, significantly inhibited U46619- and ET-1-induced Ca^{2+} sensitized force when added to β-escin-permeabilized abdominal aorta or portal vein (Fig. 6*B*). Furthermore, a recombinant C-terminal domain with a double phosphomimic mutation (S1508E/S1510E) was the most potent inhibitor of Ca^{2+} sensitization (Fig. 6*B*).

Next, we asked whether LARG and PRG might be co-recruited to the cell membrane following GPCR stimulation by a single agonist. We used mouse cerebral vessels isolated from PRG(+/−) and PRG(−/−) mice in which we were able to image individual SM cells. Immunolabeling of the TXA2 receptors clearly showed their localization at the cell periphery. Immunostaining of both PRG and LARG in PRG(+/−) mice showed diffuse cytosolic distribution of both proteins. Upon stimulation of the heterozygous cells with U46619, both PRG and LARG translocated from the cytosol to the cell periphery (Fig. 7). As expected, PRG expression was absent in the PRG(−/−) cerebral vessels, and LARG expression was unchanged. Moreover, upon stimulation with U46619, LARG relocated to the membrane.

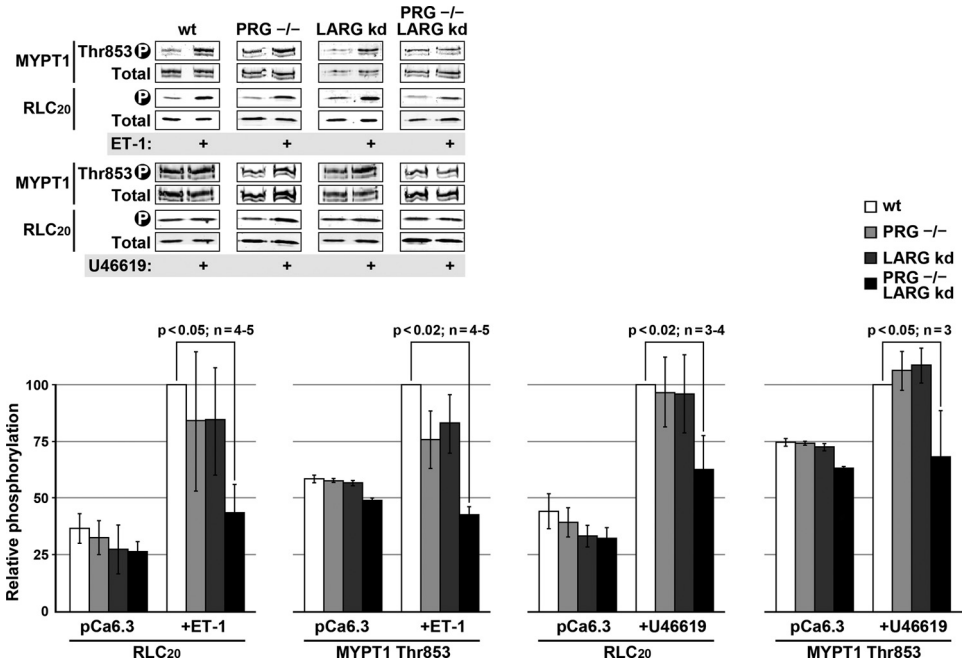

FIGURE 5. **Loss of excitatory U46619 or ET-1 Ca^{2+}-sensitized contractility of vessels from $LARG^{kd}$/PRG(−/−) mice is accompanied by a decrease in ROCK-mediated phosphorylation of myosin phosphatase at Thr-853 and RLC_{20} phosphorylation at Ser-19.** A typical Western blot analysis (*top*) and summary (*bottom*) of mouse blood vessels stimulated with 100 nM ET-1 or 300 nM U46619 are shown. The *error bars* correspond to S.E.; $n = 4–5$.

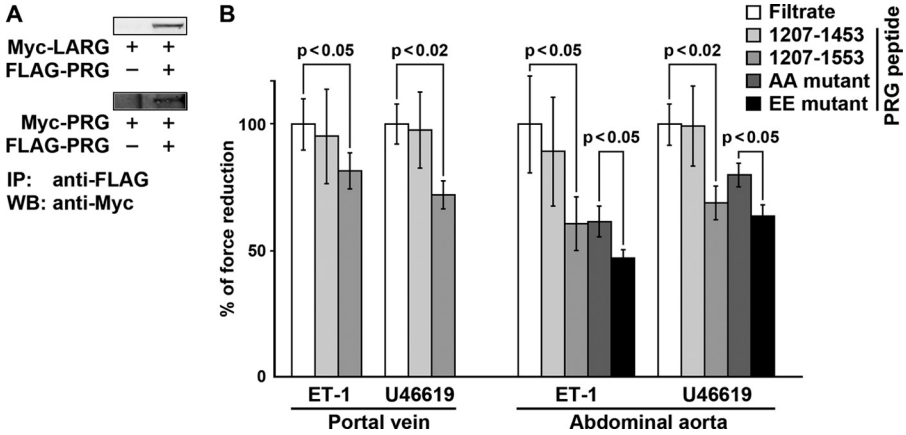

FIGURE 6. **PRG and LARG co-immunoprecipitate, and a C-terminal PRG peptide suppresses Ca^{2+}-sensitized contractility of mouse vessels consistent with hetero-oligomerization.** *A*, mammalian plasmids expressing FLAG-tagged PRG and Myc-tagged LARG were cotransfected into HEK 293T cells using Lipofectamine 2000 (Invitrogen) according to the manufacturer's protocol. After 48 h of incubation, the cells were lysed in buffer (0.5% Triton X-100, 150 mM NaCl, 50 mM Tris (pH 7.5), 2 mM EDTA, 2 mM sodium orthovanadate, 50 mM NaF, 1% protease inhibitor mixture (Sigma)) and subjected to EZview Red anti-FLAG M2 affinity gel (Sigma) for immunoprecipitation (*IP*). Western blot (*WB*) analysis was performed using anti-Myc antibody. *B*, muscles were equilibrated with the indicated peptides or their filtrate as a control for 10 min prior to agonist addition. The filtrate was without effect, indicating that the changed contractility was not due to Ca^{2+} contamination in the peptide solution. The *error bars* correspond to S.E. *AA*, S1508A/S1510A; *EE*, S1508E/S1510E.

Time Course Evolution of Ca^{2+}-sensitized Force in Normal and Genetically Altered SM—To determine how the time course evolution of Ca^{2+}-sensitized force in RhoGEF-depleted tissues compares with normal SM, we measured the kinetics of activation of Ca^{2+}-sensitized force in α-toxin-permeabilized mouse portal veins induced with U46619 and ET-1 by direct addition of the agonists to the muscle bath. Normal as well as genetically modified SM strips were used. In the case of normal SM strips, the force trace of the kinetics displayed (as expected) a slightly sigmoidal shape with a short lag phase of 32 ± 3 s for ET-1 and 21 ± 3 s for U46619. The $t_{1/2}$ was 56 ± 3 s for samples stimulated with ET-1 and 34 ± 3 s for stimulation with U46619.

Although the PRG(−/−) and $LARG^{kd}$ in α-toxin-permeabilized portal vein strips displayed maximum contraction very similar to that of normal tissues (Fig. 4), they took significantly longer to reach the maximum force, which was most apparent for ET-1 stimulation. For those stimulated by ET-1, the $t_{1/2}$ was 44 ± 3 s for WT, 61 ± 7 s for PRG(−/−), and 103 ± 12 s for $LARG^{kd}$. Unfortunately, for the PRG(−/−)/$LARG^{kd}$ samples, the contractile force was compromised to a degree that did not allow for a reliable estimate of the kinetic parameters.

Kinetics of Ca^{2+}-sensitized Force in β-Escin-permeabilized SM—To better understand the kinetics of the activation of the Ca^{2+}-sensitized force, we conducted measurements of the time course of the force development after photolysis of caged phen-

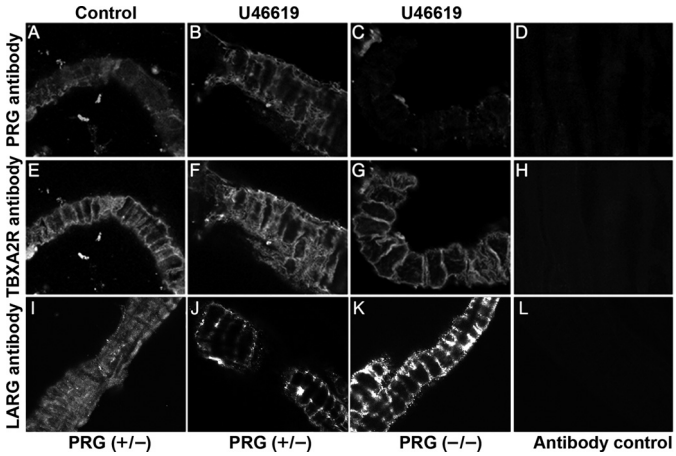

FIGURE 7. **U46619 induces translocation of PRG and LARG to a region of the plasma membrane of SM cells in mouse cerebral arteries.** The immunolabeled TXA2 receptor was localized at the SM cell surface of cerebral vessels from heterozygous PRG(+/−) and PRG(−/−) mice. Stimulation with U46619 (300 nM) for 10 min led to a translocation of the diffuse cytoplasmic signal for LARG or PRG to a defined signal at the cell surface. LARG, but not PRG, was detected at the cell surface in the PRG(−/−) vessels as expected. Secondary antibody alone gave no detectable fluorescence signal. The images (*A–L*) are representative of data from three independent experiments acquired under identical laser and power gain settings. The average diameter of an SM cell in the vessel wall is 5 μm.

ylephrine, an α_1-selective adrenergic agonist coupled to $G_{\alpha q/11}$, and after photolysis of caged GTPγS, either free and thereby acting on Gα subunits or bound to the RhoA·RhoGDI complex. The use of caged compounds circumvents diffusional delays that would contribute to the kinetic measurements. Strips from rabbit β-escin-permeabilized veins were used throughout except for caged phenylephrine, which was also assayed in α-toxin-permeabilized samples for comparison. Full contraction was first induced at *p*Ca 4.5 followed by relaxation in G1 solution (Fig. 8*A*) and then induction of ~50% of maximum contraction at *p*Ca 6.5. The samples were then transferred into the photolysis solution (*p*Ca 6.5) containing the appropriate caged substrate at the required concentration and incubated for 3 min to allow full equilibration of the caged compound throughout the muscle. A 50-ns laser pulse generated the Ca^{2+}-sensitized force, the force of which at its maximum was ~30% of the maximal force observed. In each case, the lag phase and the time required to reach half the maximum contractile force ($t_{½}$) were measured (Table 1 and Fig. 8*B*).

A series of experiments involving photolysis of caged phenylephrine at different concentrations (*i.e.* 0.25–50.0 μM) resulted in a concentration-dependent force with EC_{50} estimated at 2.5 μM. At saturating concentrations of caged phenylephrine (5.0–50.0 μM), the lag phase preceding rapid force development was 18 ± 0.8 s and was independent of [GTP] (either 1 μM or 0.5 mM). Importantly, for about 9 s, virtually no force was observed (latent phase) (Fig. 8*B*). The total time required to reach half the maximum force ($t_{½}$) induced by 5–10 μM caged phenylephrine was in the range of 40–50 s.

Experiments involving photolysis of caged GTPγS were also conducted for a range of GTPγS concentrations (0.03–6.0 μM) liberated from caged GTPγS with the force reaching a maximum at 4.0 μM where the lag phase was estimated at 15.0 ± 1.0 s and with a $t_{½}$ of 61.0 ± 7.0 s. Importantly, these results are very close within experimental error to those obtained for caged phenylephrine (Table 1).

Next, we used the photolysis of the caged GTPγS-RhoA·RhoGDI complex to initiate Ca^{2+}-sensitized force (Fig. 8*B*). Under these conditions, photolysis of caged GTPγS results in the dissociation of the complex and translocation of RhoA to the membrane, thus circumventing the action of RhoGEFs. A typical experimental force trace for contraction induced by photolysis of 25 μM caged GTPγS bound to RhoA·RhoGDI is shown in Fig. 8*B*. Contractions were examined over a range of concentrations of 0.24–6.0 μM photolyzed GTPγS-RhoA·RhoGDI (measured in the postphotolysis solution collected from the muscle trough), and the contractile force reached a maximum at 2.0 μM. The lag phase was 7 ± 0.3 s, and the $t_{½}$ was 23 ± 1.5 s (Table 1), revealing significantly faster kinetics and notably the disappearance of the latent phase.

Finally, as GTP is the natural guanosine nucleotide in this system, we initiated Ca^{2+}-sensitized force by photolysis of caged GTP bound to the constitutively active RhoA G14V·RhoGDI over a range of concentrations (0.24–6.0 μM photolyzed GTP-G14V RhoA). Contractile force saturated at 2.0 μM. This experiment yielded data very comparable with experiments using the caged GTPγS-RhoA·RhoGDI complex. The lag phase was 8 ± 1.5 s, but the $t_{½}$ was 43 ± 3.9 s presumably due to hydrolysis of GTP (Table 1). A force trace with this complex was reported in a review by us elsewhere (2) but never in a published experimental study (Fig. 3). The commonality of the short lag phase (7–8 s) with both the GTPγS- and GTP-caged complexes in contrast to that of caged phenylephrine-induced Ca^{2+}-sensitized force (18 s) further substantiates the presence of a slow rate-limiting step of ~10 s (Fig. 8*C*) upstream of the generation of RhoA-GTP. Based on studies using caged ATP, RLC_{20} phosphorylation is known to contribute only 0.2–0.5 s to the 7–8 s lag phase observed with the caged complexes (34). The remaining 6.5–7.5 s lag phase reflects the translocation of RhoA to the cell membrane, activation of ROCK, and inhibitory phosphorylation of MLCP.

Kinetics of Agonist-induced Ca^{2+}-sensitized Force in Intact SM—To assess whether the experiments involving permeabilized SM samples reflect the kinetics in intact muscles, we conducted experiments using an intact rabbit portal vein and induced full contraction using photolysis of caged phenylephrine. Release of phenylephrine induced a rapid increase in $[Ca^{2+}]_i$ at t_0 + 0.2 s that preceded force development at t_0 + 1.5 s (Fig. 9). The $[Ca^{2+}]_i$ subsequently fell and by t_0 + 15 s stabilized just above the basal $[Ca^{2+}]_i$. The force fell to a lesser degree and was followed by a secondary rise. Thus, the $[Ca^{2+}]_i$/force relationship is no longer maintained with the onset of Ca^{2+}-sensitized force. Upon pretreatment with cyclopiazonic acid to reduce the rise in $[Ca^{2+}]_i$ through inhibition of Ca^{2+} storage in the sarcoplasmic reticulum, the phenylephrine-induced Ca^{2+} transient and initial force were markedly depressed, whereas the secondary slow rise in tension was maintained (Fig. 9). As expected, the addition of the ROCK inhibitor, Y-27632 completely relaxed the secondary rise in tension (data not shown).

DISCUSSION

Many physiological agonists induce Ca^{2+}-sensitized force in SM tissues, and although their actions are mediated by specific

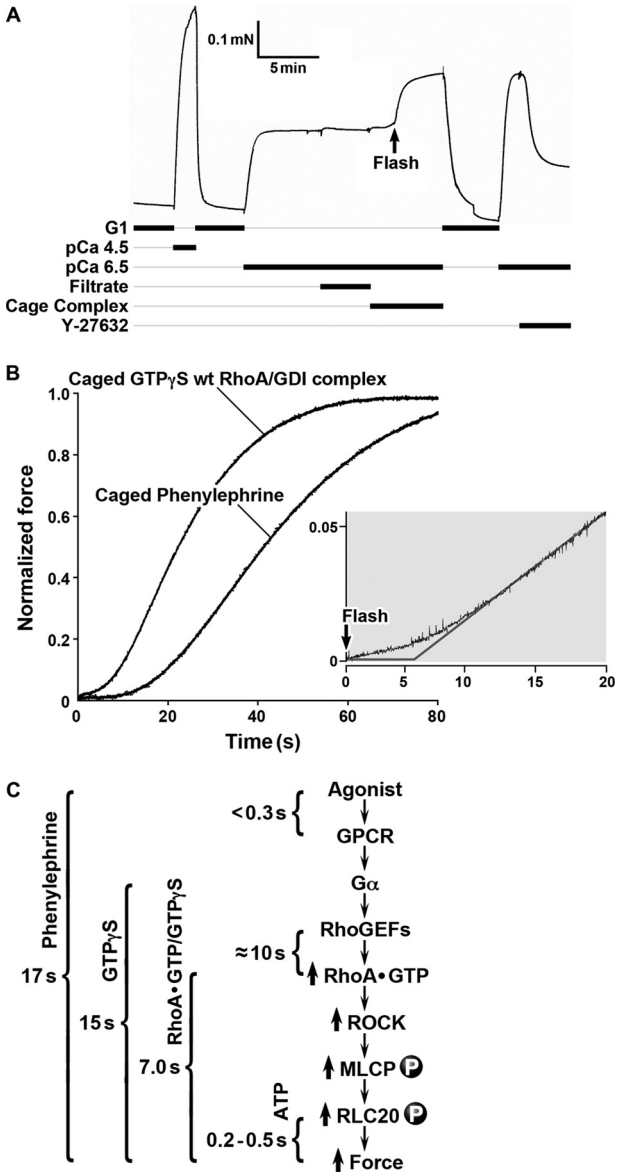

FIGURE 8. **The kinetics of force development are significantly different with photolysis of caged GTPγS-RhoA·RhoGDI complex *versus* caged phenylephrine in β-escin-permeabilized portal vein.** *A*, tension trace of the protocol used for introduction of caged compounds and their photolysis. An initial maximal contraction is induced by high [Ca^{2+}]. Following relaxation in low Ca^{2+} (G1), a partial contraction is induced by *p*Ca 6.5. Addition of filtrate or the caged complex is without effect. Following a 3-min incubation to allow penetration of the caged complex into the muscle, a 50-ns near-UV laser pulse (*Flash*) induces photolysis and Ca^{2+}-sensitized force. Following washout in G1, a rapid return to *p*Ca 6.5 gives an enhanced response, indicating that the muscle has not recovered from Ca^{2+} sensitization processes, which are relaxed by the Rho kinase inhibitor Y-27632. *B*, activation of RhoA-mediated Ca^{2+} sensitization pathway by photolysis of caged GTPγS-RhoA·RhoGDI complex using the protocol shown in *A*. Upon photolysis at t_0, 2 μM, a saturating concentration of free GTPγS-RhoA·RhoGDI, was released at a rate of 60 s^{-1}. Back-extrapolation of the fast rising phase to the prephotolysis base line (*inset*) shows a lag phase of 7 s. The lag following photolysis of caged ATP in un-prephosphorylated SM leading to RLC_{20} phosphorylation and the onset of force accounts for less than 0.5 s (34) (*C*). Thus, the 6.5-s lag phase triggered by photolysis of the complex reflects the time course of dissociation of RhoA-GDP from GDI, translocation of RhoA-GTP to the membrane, activation of ROCK, and inhibition of MLCP as shown in *C*. Photolytic release of saturating concentrations of phenylephrine (2 μM) displayed much slower kinetics than the GTPγS-RhoA·RhoGDI complex with a long delay (16 s) having a latent phase with no measurable force followed by a lag phase. The rate of force development is also significantly slower: $t_{1/2}$ is 37 s *versus* 23 s for the GTPγS-RhoA·RhoGDI complex. This slow time course reflects the events leading to activation of RhoGEFs as shown in *C*, including their translocation to the cell membrane and nucleotide exchange on RhoA-GDP·RhoGDI. *C*, agonist-induced signaling cascade for Ca^{2+}-sensitized force with the measured lag times preceding force development following photolysis of caged phenylephrine, caged GTPγS, caged GTPγS-loaded RhoA·RhoGDI complex, or caged ATP in the presence of thiophosphorylated RLC_{20}. The ~10-s difference between the lag times for caged phenylephrine or caged GTPγS *versus* GTPγS-loaded RhoA·RhoGDI complex reflects the processes underlying the activation of RhoGEFs. *mN*, millinewtons.

TABLE 1

Lag phases and $t_{1/2}$ values for Ca^{2+}-sensitized force at saturating concentrations of caged ligands

n.s., not significant; wt, wild-type.

Caged Ligands	Permeabilization	Lag phase (sec ± SEM)	$t_{1/2}$ (sec ± SEM)
Phenylephrine	α-toxin	16 ± 1.6	37 ± 3.8
	β-escin	18 ± 0.8	43 ± 1.1
GTPγS	β-escin	15 ± 1.0	61 ± 7.1
GTPγS-wtRhoA/RhoGDI	β-escin	7 ± 0.3	23 ± 1.5
GTP-G14VRhoA/RhoGDI	β-escin	8 ± 1.5	43 ± 3.9

n.s. between Phenylephrine (α-toxin) 16 ± 1.6 and Phenylephrine (β-escin) 18 ± 0.8; n.s. between Phenylephrine (α-toxin) 37 ± 3.8 and Phenylephrine (β-escin) 43 ± 1.1; p<0.001 between GTPγS 15 ± 1.0 and GTPγS-wtRhoA/RhoGDI 7 ± 0.3; p<0.001 between Phenylephrine (β-escin) 18 ± 0.8 and GTP-G14VRhoA/RhoGDI 8 ± 1.5; p<0.002 between GTPγS-wtRhoA/RhoGDI 7 ± 0.3 and GTP-G14VRhoA/RhoGDI 8 ± 1.5; n.s. between GTPγS-wtRhoA/RhoGDI 7 ± 0.3 and GTP-G14VRhoA/RhoGDI 8 ± 1.5; p<0.001 between GTPγS 61 ± 7.1 and GTPγS-wtRhoA/RhoGDI 23 ± 1.5; p<0.001 between GTPγS-wtRhoA/RhoGDI 23 ± 1.5 and GTP-G14VRhoA/RhoGDI 43 ± 3.9.

GPCRs, downstream signaling may occur through degenerate networks as GPCRs can couple to various Gα subunits of heterotrimeric G-protein, which in turn may potentially activate one or more RhoGEFs, catalyzing nucleotide exchange on RhoA. In this study, we investigated the possibility of concerted, cooperative activity of two such RhoGEFs, *i.e.* LARG and PRG. Unlike many other studies that use cultured SM cells, we used intact and permeabilized blood vessels that were genetically depleted in PRG and LARG. Because a double knock-out in mice causes embryonic lethality (18), we turned to a different approach of silencing the LARG gene in intact organ-cultured tissues isolated from the PRG(−/−) mouse. This technique yielded samples in which LARG was reduced by ~65%, whereas PRG was obviously absent. Importantly, mRNA screens and Westerns blots indicated that the knock-out of PRG did not noticeably disrupt the expression patterns of other RhoGEFs that potentially might bias the experiments.

We targeted PRG and LARG because both act downstream of $G\alpha_{12}$ and $G\alpha_{13}$ with which they interact through a dedicated domain known as the regulator of G-protein signaling-like domain (35), and both have been found by us and others to be expressed in SM (36, 37). We assayed the RhoA-mediated Ca^{2+}-sensitized component of the SM contractile force induced by two potent vasoconstricting agonists, *i.e.* ET-1 and U46619, a stable analog of thromboxane A2.

Interestingly, the knock-out of PRG or depletion of LARG through silencing had little effect on the maximum contractile force when compared with normal portal vein SM tissue, and the reduction of force was statistically significant only when ET-1 was used as agonist. In contrast, samples in which PRG was knocked out and LARG was depleted showed a dramatic and reproducible phenotype in which contractile force was reduced to <50% when U46619 was used and to <25% with ET-1 stimulation. These results strongly suggest that both RhoGEFs are activated by each of the two agonists, and each RhoGEF is capable of generating a high or maximal level of Ca^{2+}-sensitized force. This is further supported by our finding

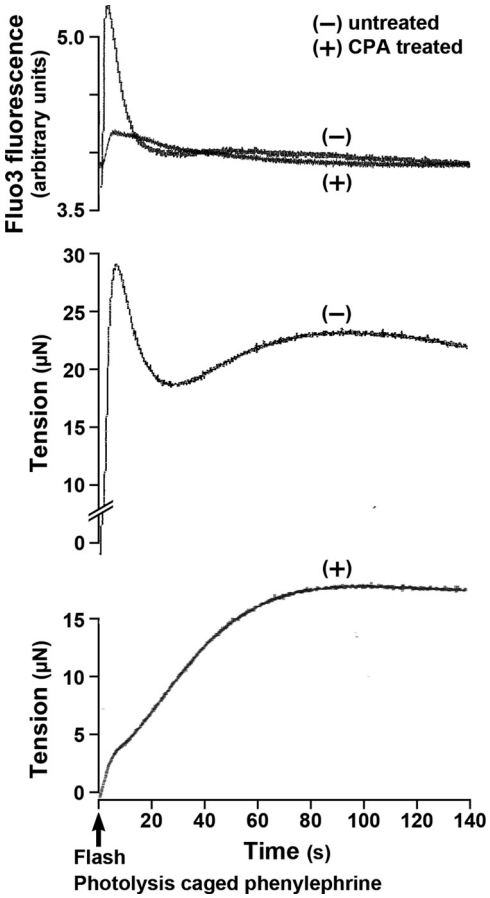

FIGURE 9. **Phenylephrine-induced force in intact portal vein consists of an initial phasic component preceded by a cyclopiazonic acid-sensitive Ca^{2+} transient and a secondary tonic force component at near basal $[Ca^{2+}]$.** Vessels were loaded with Fluo3 and activated by photolytic release (*arrow*) of ~1.5 μM phenylephrine from 20 μM caged phenylephrine. Cyclopiazonic acid (*CPA*) treatment used to reduce Ca^{2+} uptake into the sarcoplasmic reticulum markedly suppressed the Ca^{2+} response and the initial force transient but not the secondary rise in force.

that both PRG and LARG translocated to the SM cell membrane region upon stimulation with U46619.

Although in our experiments we targeted RhoGEFs that are expected to be activated primarily by $G\alpha_{12/13}$, some caution must be exercised in the interpretation of the results. First, the strictly G_q-coupled histamine receptor has been shown to activate LARG (38). Also, it is not clear that TXA2 and ET-1 signal exclusively through $G\alpha_{12/13}$. It is widely believed that the Ca^{2+}-sensitizing function of TXA2 is mediated by $G\alpha_{12/13}$, but it is also known that $G_{q/11}$ may be activated by the TXA2 receptor in which case the p63RhoGEF could be activated. However, this is unlikely as we have previously shown that the silencing of p63RhoGEF in mouse portal vein had no effect of U46619-induced Ca^{2+}-sensitized force but did suppress the ET-1 response (11). Similarly, ET-1 has been shown to cause transient Ca^{2+}-induced contraction through G_q-coupled receptors, whereas the Ca^{2+}-sensitized force is mediated by $G\alpha_{13}$ coupling (39). Thus, the G_q/p63RhoGEF coupling is also possible with ET-1 stimulation. These degenerate signaling networks may easily explain why a significant fraction of sensitized force was still observed after the PRG knock-out and LARG silencing. We also note that the silencing depleted ~70% of LARG, so one would expect that the LARG pathway is still active in the modified samples. Whatever the source of the residual force in the PRG/LARG-depleted samples, it is the combined effect of these two RhoGEFs that is responsible for Ca^{2+}-sensitized force induced by either ET-1 or U46619, and both translocate to the membrane following stimulation by U46619.

$G\alpha_{12/13}$-LARG has already been implicated in salt-mediated hypertension in mouse models (9). In that study, the authors noted that both PRG and LARG are present in murine SM but discounted the role of PRG due to its lower copy numbers present. Interestingly, a deficiency of both PRG and LARG, but not either alone, results in defective embryonic development, supporting an essential developmental role for both of these GEFs (18). Here we propose, based on our experimental evidence, that PRG is almost equally important for RhoA activation. Is important to note that PRG and LARG are catalytically very potent, and this could compensate for low levels (40, 41). Even more significant is the observation that PRG and LARG heterodimerize in cells (33). In concert, we showed that both RhoGEFs, not only LARG, are detectably translocated to the cell membrane in murine cerebral vessels stimulated with U46619. This co-recruitment could be due to direct activation and co-recruitment of PRG in a heterodimer with LARG. However, the isolated recombinant C-domain of PRG, which is responsible for heterodimerization with LARG, was able to inhibit the Ca^{2+}-sensitized force, attesting to the fact that dimerization makes a significant contribution to the co-recruitment.

Another important observation in our study is that the depletion of either PRG or LARG impaired the kinetics of the ET-1-induced Ca^{2+}-sensitized force, significantly extending the half-time required to reach full contraction. This indicates that although either of the RhoGEFs can generate nearly full contraction (especially in the U46619-stimulated samples) the rate by which RhoA activation is saturated becomes the limiting factor. This observation is consistent with the fact that in general terms RhoGEFs are relatively poor catalysts, and the nucleotide exchange reaction may take minutes or even longer *in vivo* to activate available RhoA.

Given the impact the RhoGEFs have on the kinetics of Ca^{2+}-sensitized force development, we wondered whether we could probe more deeply into the process. Unfortunately, murine portal vein and other vessels present considerable challenge for experimental studies, and β-escin permeabilization necessary for the introduction of caged complexes fails to produce samples in which Ca^{2+}-sensitized force can be reliably monitored. We were therefore limited in our studies to larger portal veins obtained from rabbits that give highly reproducible contractions and for which receptor coupling is conserved with β-escin permeabilization. We asked what differences could be observed in force kinetics between the Ca^{2+}-sensitized components induced by stimulation of the vasoconstricting agonist receptor, direct stimulation of Gα subunits, and direct activation of RhoA, circumventing the RhoGEFs. Laser photolysis was used to activate caged phenylephrine, caged GTPγS, and the caged GTPγS-RhoA·RhoGDI and caged GTP-G14V RhoA complexes. In this way, we eliminated diffusional effects. Although we used caged phenylephrine (caged ET-1 and U46619 are not available), which is coupled to $G\alpha_{q/11}$ and not $G\alpha_{12/13}$, we

assumed that the kinetics of the response will be generally the same as for isolated $G\alpha_{12/13}$. However, the underlying mechanisms responsible for the slow GEF activation for the different stimuli may differ. For example, $G\alpha_{q/11}$-coupled p63RhoGEF is palmitoylated and when expressed is found at the cell surface (42, 43), whereas we found that LARG and PRG translocated from the cytoplasm to the SM cell surface in cerebral vessels stimulated with U46619 stimulation (Fig. 7). The lag phase and $t_{1/2}$ for force stimulated by photolysis of phenylephrine and caged GTPγS are almost identical, consistent with the fact that the signaling between receptors and Gα proteins is on a subsecond scale. Receptor/G-protein interaction is maximal in about 50 ms (44), and activation of Gα subunits of GPCRs is also fast with a half-time of activation of $G\alpha_q$ of 350 ms (45) and of G_s and G_i of 450 and 690 ms, respectively (46, 47). In contrast, we observed a marked difference between the kinetics of the Ca^{2+}-sensitized response to photolysis of caged GTPγS and to the release of GTPγS-RhoA or GTP-G14V RhoA from the complex with RhoGDI (Fig. 8*C* and Table 1). The lag phase was shortened from 15 to 7 s. The shorter $t_{1/2}$ may in part be an artifact due to the larger amount of active RhoA translocated to the membrane in experiments where the recombinant RhoA·RhoGDI complex was introduced as opposed to activation of endogenous RhoA only. The long delay of contraction induced by photolysis of caged phenylephrine (16 s) includes a latent phase with no measurable force (Fig. 8, *B* and *C*) and a lag phase, which hints at cooperativity at an early stage of force development. This reflects events leading to the activation of RhoGEFs, including their translocation to the plasma membrane, and nucleotide exchange on RhoA-GDP·RhoGDI. The cooperative effect may be due at least in part to the recently discovered positive feedback loop whereby the activated, GTP-bound RhoA binds to the PH (pleckstrin homology) domains of RhoGEFs of the Lbc family, which includes PRG and LARG, increasing turnover of basal RhoA activity by as much as 40-fold (48). Another reason for the sigmoidal curve of the kinetics is concentration enhancement effects. The clustering of receptors and signaling molecules in scaffolds at the membrane is critical for increasing the local concentrations as well as amplification of steps in signal transduction cascades (49).

Clearly, the significantly delayed contraction of SM tissues with depleted PRG or LARG is fully consistent with this picture of Ca^{2+}-sensitized force kinetics even though the two models used in our studies are not fully comparable. In conclusion, we have shown that both PRG and LARG are activated in SM tissues stimulated with $G\alpha_{12/13}$-coupled physiologically and pathophysiologically important thromboxane A2 and endothelin-1 receptor agonists ET-1 and U46619 and that RhoGEF activation plays an important role in the delay of Ca^{2+}-sensitized, sustained force with respect to the initial Ca^{2+}-induced transient.

Acknowledgments—We thank Natalya Olekhnovich for technical assistance and Dr. Alexander Khromov for the aci-nitro analysis of the photolysis kinetics. The gifts of caged phenylephrine, caged GTP (R-isomer), and S-caged GTPγS from Jeffery Walker, Gordon Reid, and John Corrie are gratefully acknowledged. John Corrie is also acknowledged for helpful discussions.

REFERENCES

1. Somlyo, A. P., and Somlyo, A. V. (1994) Signal transduction and regulation in smooth muscle. *Nature* **372,** 231–236
2. Somlyo, A. P., and Somlyo, A. V. (2003) Ca^{2+} sensitivity of smooth muscle and nonmuscle myosin II: modulated by G proteins, kinases, and myosin phosphatase. *Physiol. Rev.* **83,** 1325–1358
3. Hong, F., Haldeman, B. D., Jackson, D., Carter, M., Baker, J. E., and Cremo, C. R. (2011) Biochemistry of smooth muscle myosin light chain kinase. *Arch. Biochem. Biophys.* **510,** 135–146
4. Kimura, K., Ito, M., Amano, M., Chihara, K., Fukata, Y., Nakafuku, M., Yamamori, B., Feng, J., Nakano, T., Okawa, K., Iwamatsu, A., and Kaibuchi, K. (1996) Regulation of myosin phosphatase by Rho and Rho-associated kinase (Rho-kinase). *Science* **273,** 245–248
5. Ichikawa, K., Ito, M., and Hartshorne, D. J. (1996) Phosphorylation of the large subunit of myosin phosphatase and inhibition of phosphatase activity. *J. Biol. Chem.* **271,** 4733–4740
6. Wettschureck, N., and Offermanns, S. (2002) Rho/Rho-kinase mediated signaling in physiology and pathophysiology. *J. Mol. Med.* **80,** 629–638
7. Rossman, K. L., Der, C. J., and Sondek, J. (2005) GEF means go: turning on RHO GTPases with guanine nucleotide-exchange factors. *Nat. Rev. Mol. Cell Biol.* **6,** 167–180
8. Jaiswal, M., Dvorsky, R., and Ahmadian, M. R. (2013) Deciphering the molecular and functional basis of Dbl family proteins: a novel systematic approach toward classification of selective activation of the Rho family proteins. *J. Biol. Chem.* **288,** 4486–4500
9. Wirth, A., Benyó, Z., Lukasova, M., Leutgeb, B., Wettschureck, N., Gorbey, S., Orsy, P., Horváth, B., Maser-Gluth, C., Greiner, E., Lemmer, B., Schütz, G., Gutkind, J. S., and Offermanns, S. (2008) G12-G13-LARG-mediated signaling in vascular smooth muscle is required for salt-induced hypertension. *Nat. Med.* **14,** 64–68
10. Wuertz, C. M., Lorincz, A., Vettel, C., Thomas, M. A., Wieland, T., and Lutz, S. (2010) p63RhoGEF—a key mediator of angiotensin II-dependent signaling and processes in vascular smooth muscle cells. *FASEB J.* **24,** 4865–4876
11. Momotani, K., Artamonov, M. V., Utepbergenov, D., Derewenda, U., Derewenda, Z. S., and Somlyo, A. V. (2011) p63RhoGEF couples $G\alpha_{q/11}$-mediated signaling to Ca^{2+} sensitization of vascular smooth muscle contractility. *Circ. Res.* **109,** 993–1002
12. Momotani, K., and Somlyo, A. V. (2012) p63RhoGEF: a new switch for G_q-mediated activation of smooth muscle. *Trends Cardiovasc. Med.* **22,** 122–127
13. Fukuhara, S., Chikumi, H., and Gutkind, J. S. (2000) Leukemia-associated Rho guanine nucleotide exchange factor (LARG) links heterotrimeric G proteins of the G_{12} family to Rho. *FEBS Lett.* **485,** 183–188
14. Fukuhara, S., Murga, C., Zohar, M., Igishi, T., and Gutkind, J. S. (1999) A novel PDZ domain containing guanine nucleotide exchange factor links heterotrimeric G proteins to Rho. *J. Biol. Chem.* **274,** 5868–5879
15. Kozasa, T., Jiang, X., Hart, M. J., Sternweis, P. M., Singer, W. D., Gilman, A. G., Bollag, G., and Sternweis, P. C. (1998) p115 RhoGEF, a GTPase activating protein for $G\alpha_{12}$ and $G\alpha_{13}$. *Science* **280,** 2109–2111
16. Longenecker, K. L., Lewis, M. E., Chikumi, H., Gutkind, J. S., and Derewenda, Z. S. (2001) Structure of the RGS-like domain from PDZ-RhoGEF: linking heterotrimeric G protein-coupled signaling to Rho GTPases. *Structure* **9,** 559–569
17. Guilluy, C., Brégeon, J., Toumaniantz, G., Rolli-Derkinderen, M., Retailleau, K., Loufrani, L., Henrion, D., Scalbert, E., Bril, A., Torres, R. M., Offermanns, S., Pacaud, P., and Loirand, G. (2010) The Rho exchange factor Arhgef1 mediates the effects of angiotensin II on vascular tone and blood pressure. *Nat. Med.* **16,** 183–190
18. Mikelis, C. M., Palmby, T. R., Simaan, M., Li, W., Szabo, R., Lyons, R., Martin, D., Yagi, H., Fukuhara, S., Chikumi, H., Galisteo, R., Mukouyama, Y., Bugge, T. H., and Gutkind, J. S. (2013) PDZ-RhoGEF and LARG are essential for embryonic development and provide a link between thrombin and LPA receptors and Rho activation. *J. Biol. Chem.* **288,** 12232–12243
19. Yoshida, T., Sinha, S., Dandré, F., Wamhoff, B. R., Hoofnagle, M. H., Kremer, B. E., Wang, D. Z., Olson, E. N., and Owens, G. K. (2003) Myocardin

is a key regulator of CArG-dependent transcription of multiple smooth muscle marker genes. *Circ. Res.* **92,** 856–864
20. Somlyo, A. V., Horiuti, K., Trentham, D. R., Kitazawa, T., and Somlyo, A. P. (1992) Kinetics of Ca^{2+} release and contraction induced by photolysis of caged D-*myo*-inositol 1,4,5-trisphosphate in smooth muscle. The effects of heparin, procaine, and adenine nucleotides. *J. Biol. Chem.* **267,** 22316–22322
21. Somlyo, A. V., Goldman, Y. E., Fujimori, T., Bond, M., Trentham, D. R., and Somlyo, A. P. (1988) Cross-bridge kinetics, cooperativity, and negatively strained cross-bridges in vertebrate smooth muscle. A laser-flash photolysis study. *J. Gen. Physiol.* **91,** 165–192
22. Goldman, Y. E., Hibberd, M. G., and Trentham, D. R. (1984) Initiation of active contraction by photogeneration of adenosine-5′-triphosphate in rabbit psoas muscle fibres. *J. Physiol.* **354,** 605–624
23. McCray, J. A., and Trentham, D. R. (1989) Properties and uses of photoreactive caged compounds. *Annu. Rev. Biophys. Biophys. Chem.* **18,** 239–270
24. Read, P. W., Liu, X., Longenecker, K., Dipierro, C. G., Walker, L. A., Somlyo, A. V., Somlyo, A. P., and Nakamoto, R. K. (2000) Human RhoA/RhoGDI complex expressed in yeast: GTP exchange is sufficient for translocation of RhoA to liposomes. *Protein Sci.* **9,** 376–386
25. Scheidig, A. J., Franken, S. M., Corrie, J. E., Reid, G. P., Wittinghofer, A., Pai, E. F., and Goody, R. S. (1995) X-ray crystal structure analysis of the catalytic domain of the oncogene product $p21^{H\text{-}ras}$ complexed with caged GTP and mant dGppNHp. *J. Mol. Biol.* **253,** 132–150
26. Corrie, J. E. T., Reid, G.P., Trentham, D.R., Hursthouse, M.B., and Mazid, M.A. (1992) Synthesis and absolute stereochemistry of the two diastereoisomers of P_3-1-(2-nitrophenyl)ethyl adenosine triphosphate ('caged ATP'). *J. Chem. Soc. Perkin Trans.* **1,** 1015–1019
27. Sheffield, P., Garrard, S., and Derewenda, Z. (1999) Overcoming expression and purification problems of RhoGDI using a family of "parallel" expression vectors. *Protein Expr. Purif.* **15,** 34–39
28. Neppl, R. L., Lubomirov, L. T., Momotani, K., Pfitzer, G., Eto, M., and Somlyo, A. V. (2009) Thromboxane A2-induced bi-directional regulation of cerebral arterial tone. *J. Biol. Chem.* **284,** 6348–6360
29. Walker, J. W., and Trentham, D. R. (1988) Caged phenylephrine synthesis and photochemical properties. *Biophys. J.* **53,** A596
30. Walker, J. W., Martin, H., Schmitt, F. R., and Barsotti, R. J. (1993) Rapid release of an α-adrenergic receptor ligand from photolabile analogs. *Biochemistry* **32,** 1338–1345
31. Walker, J. W., Reid, G. P., and Trentham, D. R. (1989) Synthesis and properties of caged nucleotides. *Methods Enzymol.* **172,** 288–301
32. Grabocka, E., and Wedegaertner, P. B. (2007) Disruption of oligomerization induces nucleocytoplasmic shuttling of leukemia-associated Rho guanine-nucleotide exchange factor. *Mol. Pharmacol.* **72,** 993–1002
33. Chikumi, H., Barac, A., Behbahani, B., Gao, Y., Teramoto, H., Zheng, Y., and Gutkind, J. S. (2004) Homo- and hetero-oligomerization of PDZ-RhoGEF, LARG and p115RhoGEF by their C-terminal region regulates their *in vivo* Rho GEF activity and transforming potential. *Oncogene* **23,** 233–240
34. Horiuti, K., Somlyo, A. V., Goldman, Y. E., and Somlyo, A. P. (1989) Kinetics of contraction initiated by flash photolysis of caged adenosine triphosphate in tonic and phasic smooth muscles. *J. Gen. Physiol.* **94,** 769–781
35. Chen, Z., Singer, W. D., Sternweis, P. C., and Sprang, S. R. (2005) Structure of the p115RhoGEF rgRGS domain-Gα13/i1 chimera complex suggests convergent evolution of a GTPase activator. *Nat. Struct. Mol. Biol.* **12,** 191–197
36. Cario-Toumaniantz, C., Ferland-McCollough, D., Chadeuf, G., Toumaniantz, G., Rodriguez, M., Galizzi, J. P., Lockhart, B., Bril, A., Scalbert, E., Loirand, G., and Pacaud, P. (2012) RhoA guanine exchange factor expression profile in arteries: evidence for a Rho kinase-dependent negative feedback in angiotensin II-dependent hypertension. *Am. J. Physiol. Cell Physiol.* **302,** C1394–C1404
37. Derewenda, U., Oleksy, A., Stevenson, A. S., Korczynska, J., Dauter, Z., Somlyo, A. P., Otlewski, J., Somlyo, A. V., and Derewenda, Z. S. (2004) The crystal structure of RhoA in complex with the DH/PH fragment of PDZRhoGEF, an activator of the Ca^{2+} sensitization pathway in smooth muscle. *Structure* **12,** 1955–1965
38. Pfreimer, M., Vatter, P., Langer, T., Wieland, T., Gierschik, P., and Moepps, B. (2012) LARG links histamine-H1-receptor-activated Gq to Rho-GTPase-dependent signaling pathways. *Cell. Signal.* **24,** 652–663
39. Gohla, A., Schultz, G., and Offermanns, S. (2000) Role for G_{12}/G_{13} in agonist-induced vascular smooth muscle cell contraction. *Circ. Res.* **87,** 221–227
40. Oleksy, A., Opaliński, Ł., Derewenda, U., Derewenda, Z. S., and Otlewski, J. (2006) The molecular basis of RhoA specificity in the guanine nucleotide exchange factor PDZ-RhoGEF. *J. Biol. Chem.* **281,** 32891–32897
41. Jaiswal, M., Gremer, L., Dvorsky, R., Haeusler, L. C., Cirstea, I. C., Uhlenbrock, K., and Ahmadian, M. R. (2011) Mechanistic insights into specificity, activity and regulatory elements of the RGS-containing Rho-specific guanine nucleotide exchange factors p115, PDZ-RhoGEF (PRG) and leukemia-associated RhoGEF (LARG). *J. Biol. Chem.* **286,** 18202–18212
42. Aittaleb, M., Nishimura, A., Linder, M. E., and Tesmer, J. J. (2011) Plasma membrane association of p63 Rho guanine nucleotide exchange factor (p63RhoGEF) is mediated by palmitoylation and is required for basal activity in cells. *J. Biol. Chem.* **286,** 34448–34456
43. Shankaranarayanan, A., Boguth, C. A., Lutz, S., Vettel, C., Uhlemann, F., Aittaleb, M., Wieland, T., and Tesmer, J. J. (2010) Gαq allosterically activates and relieves autoinhibition of p63RhoGEF. *Cell. Signal.* **22,** 1114–1123
44. Hein, P., Frank, M., Hoffmann, C., Lohse, M. J., and Bünemann, M. (2005) Dynamics of receptor/G protein coupling in living cells. *EMBO J.* **24,** 4106–4114
45. Adjobo-Hermans, M. J., Goedhart, J., van Weeren, L., Nijmeijer, S., Manders, E. M., Offermanns, S., and Gadella, T. W. (2011) Real-time visualization of heterotrimeric G protein Gq activation in living cells. *BMC Biol.* **9,** 32
46. Bünemann, M., Frank, M., and Lohse, M. J. (2003) Gi protein activation in intact cells involves subunit rearrangement rather than dissociation. *Proc. Natl. Acad. Sci. U.S.A.* **100,** 16077–16082
47. Hein, P., Rochais, F., Hoffmann, C., Dorsch, S., Nikolaev, V. O., Engelhardt, S., Berlot, C. H., Lohse, M. J., and Bünemann, M. (2006) Gs activation is time-limiting in initiating receptor-mediated signaling. *J. Biol. Chem.* **281,** 33345–33351
48. Medina, F., Carter, A. M., Dada, O., Gutowski, S., Hadas, J., Chen, Z., and Sternweis, P. C. (2013) Activated RhoA is a positive feedback regulator of the Lbc family of Rho guanine nucleotide exchange factor proteins. *J. Biol. Chem.* **288,** 11325–11333
49. Groves, J. T., and Kuriyan, J. (2010) Molecular mechanisms in signal transduction at the membrane. *Nat. Struct. Mol. Biol.* **17,** 659–665